

HYPERION (S VII): SHAPE AND MAPS OF THE SATURNIAN SATELLITE. M. V. Nyrtsov¹, A. I. Sokolov¹, M. E. Fleis², A. E. Zubarev³, N. A. Kozlova³, ¹Lomonosov Moscow State University, 119991, Leninskiye Gory, 1, Moscow, Russia (nyrtsovmaxim@gmail.com), ²Institute of Geography, Russian Academy of Sciences, 119017, Staromonetnyi Lane, 29, Moscow, Russia (fleis.maria@yandex.ru), ³Moscow State University of Geodesy and Cartography (MIIGAiK), 105064, Gorokhovskiy per, 4, Moscow, Russia (mexlab@miigaik.ru).

Introduction: On August 22, 2017, the spacecraft Cassini sent back the final batch of images of Saturn's natural moon Hyperion (S VII). These images had a resolution starting at 20 meters per pixel. Even with these new high-resolution data Hyperion appeared to be a challenge for planetary cartography.

First challenge is the irregular shape of its body, close to a triaxial ellipsoid, which does not allow us to use standard cartographic projections and software packages. Second reason is Hyperion's chaotic rotation [1-4]. With the proof of the fact of its chaotic rotation, the IAU stopped assigning names to objects and recording them. Despite this, descriptions of various unnamed craters appear in published papers [5], [6], etc.

Moreover, Hyperion does not have an established coordinate system. Hyperion has not been mentioned in IAU reports since 1990. The 1979 IAU Report suggests using a sphere with a radius of $R=112$ km for mapping, however, this was even before the Voyagers approached Hyperion in 1980, 1981. Then there are references to 5 named objects on its surface. The Gazetteer of Planetary Nomenclature provides directions of axis counting. This is all the information available.

Hyperion CPN, DEM, and mosaic: Processing of best 166 new Cassini images allowed us to cover whole Hyperion surface and create a new Control Point Network (CPN) of more than 2,000 points. On this basis, we established a reference frame working model for Hyperion, useful for new estimates of shape parameters and follow-up mapping. Due to its chaotic rotation the best fit ellipsoid for Hyperion was determined, derived under the condition of minimum deviation from the physical surface, without taking into account the physical parameters of rotation and center of mass. Consequently, we find best-fit ellipsoid parameters of $180.9 \times 129.0 \times 102.0$ km as well as new estimates for bulk density of 565 kg/km^3 [7], which is ~4% more than the values previously obtained by other researchers [8], [9]. To set the coordinate system, geometric axes were selected. Based on the new CPN and reference frame, global mapping products have been created, which included a gridded DEM (Fig. 1) and an orthomosaic (best resolution: 50 m/pixel).

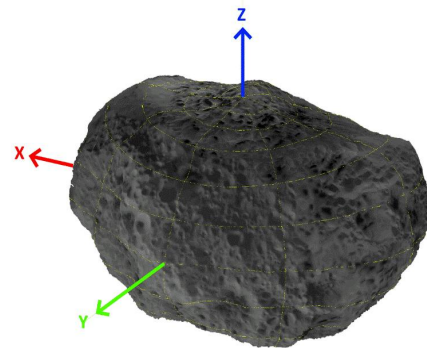


Fig. 1. Created Hyperion DEM with shown axes of suggested coordinate system

Cartography and mapping: Based on the created orthophotomosaic and DEM of the satellite surface, its mapping was performed in various projections.

Of more than a hundred Saturnian moons, only 24 have regular rotation, the most of the rest are retrograde, that is why West longitudes are used for them. Thus, the direction of their rotation is different from the direction of rotation of the central body (Saturn). In the case of Hyperion with chaotic rotation (the study shows that Hyperion body “turns over” from time to time) we cannot determine East and West directions in the same way as it is usually done. So, we chose for mapping Hyperion's axes +East to emphasize the difference between Hyperion and such Saturnian satellites as Enceladus, Dione, etc.

Hyperion map in meridian section projections of the triaxial ellipsoid. As Hyperion body is far from sphere shape, we used determined parameters of the triaxial ellipsoid for mapping.

The choice of projection and map layout is primarily related to the ability to preserve the shape of relief features on the compiled map by minimizing angular distortions [10]. In addition, the map shows that the constructed contour lines are in good agreement with the ortho mosaic (Fig. 2). Thus, the selected triaxial ellipsoid is optimal for approximating the figure of this celestial body.

In addition, the cylindrical and azimuthal projections of the meridian section [11] in the proposed layout are quite recognizable, and the decrease in the distance from the equator to the parallel

with a given latitude with increasing longitude from 0° to 90° in the cylindrical projection clearly demonstrates equatorial compression. To plot contour lines on the map, geodetic heights relative to a triaxial ellipsoid were calculated [10].

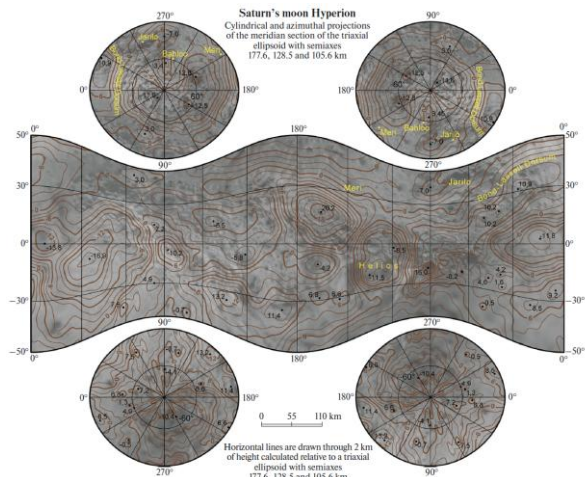


Fig. 2. Hyperion map in meridian section projection

Hyperion map in equal-area projection of the triaxial ellipsoid. As we have a digital elevation model, we calculated geodetic heights relative to the triaxial ellipsoid and displayed them on a hypsometric map in equal-area projection (Fig. 3), which allows us to compare surface areas occupied by specific heights [12]. A calculated hypsogram (Fig. 4) showed a normal distribution of heights, with a peak in the center, that proves the quality of determined ellipsoid parameters and orientation.

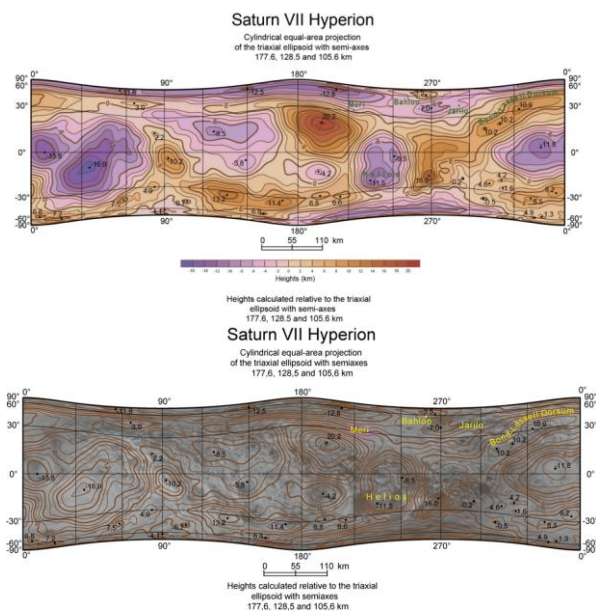


Fig. 3. Hyperion maps in equal-area projection

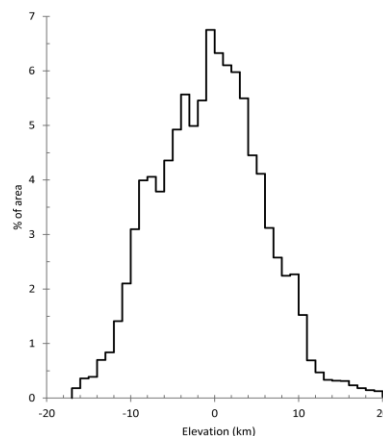


Fig. 4. Hypsogram of Hyperion heights distribution

Conclusions: Also, the constructed hypsograms can be used to select a scale when creating a hypsometric map of a celestial body. For larger area altitude ranges, a more frequent scale may be recommended.

Acknowledgments: The cartographic part of the article was carried out according to State assignments No. 121051400061-9 (A.I. Sokolov, M.V. Nyrtsov) and FMWS-2024-0009 No. 1023032700199-9 (M.E. Fleis). The image data processing and shape study (A.E. Zubarev, N.A. Kozlova) was performed according to State assignments no. 124071100067-9 (FSFE-2024-0001).

References: [1] Tarnopolski M. (2017) *A&A*, 606, A43. [2] Wisdom J. et al. (1984) *Icarus* 58, 137–152. [3] Melnikov A.V (2016), *Astr.&neb.mex.* 238 c. (in Russian). [4] Melnikov A.V (2020) *SSR*, 54, 432-441. [5] Howard et al. (2012), *Icarus* 220, 268-276. [6] Daltom III et al. (2012) *Icarus* 220, 752-776. [7] Zubarev A.E. and Nadezhdina I.E. (2025) *Icarus* (in press). [8] Thomas P.C., et al. (2007) *Nature* 448, 50. [9] Jacobson R.A. (2022) *AJ* 164, 199. [10] Sokolov A.I. et al. (2024) *SSR* 58, 112–121. [11] Nyrtsov M.V. et al. (2021) *Geodezia i kartografia* 82, 11-22. [12] Sokolov et al. (2024) *PSS* 249, 10594.